Original Article

# Comparison of Color Fundus Photography, Infrared Fundus Photography, and Optical Coherence Tomography in Detecting Retinal Hamartoma in Patients with Tuberous Sclerosis Complex

**Da-Yong Bai[1,2], Xu Wang[3], Jun-Yang Zhao[1], Li Li[1], Jun Gao[4], Ning-Li Wang[2]**

[1]Department of Ophthalmology, Beijing Children's Hospital, Capital Medical University, Beijing 100045, China
[2]Beijing Institute of Ophthalmology, Beijing Tongren Eye Center, Beijing Tongren Hospital, Capital Medical University, Beijing Ophthalmology and Visual Science Key Laboratory, Beijing 100730, China
[3]Department of Neurology, Beijing Children's Hospital, Capital Medical University, Beijing 100045, China
[4]Department of Radiology, Beijing Children's Hospital, Capital Medical University, Beijing 100045, China

## Abstract

**Background:** A sensitive method is required to detect retinal hamartomas in patients with tuberous sclerosis complex (TSC). The aim of the present study was to compare the color fundus photography, infrared imaging (IFG), and optical coherence tomography (OCT) in the detection rate of retinal hamartoma in patients with TSC.
**Methods:** This study included 11 patients (22 eyes) with TSC, who underwent color fundus photography, IFG, and spectral-domain OCT to detect retinal hamartomas. *TSC1* and *TSC2* mutations were tested in eight patients.
**Results:** The mean age of the 11 patients was 8.0 ± 2.1 years. The mean spherical equivalent was −0.55 ± 1.42 D by autorefraction with cycloplegia. In 11 patients (22 eyes), OCT, infrared fundus photography, and color fundus photography revealed 26, 18, and 9 hamartomas, respectively. The predominant hamartoma was type I (55.6%). All the hamartomas that detected by color fundus photography or IFG can be detected by OCT.
**Conclusion:** Among the methods of color fundus photography, IFG, and OCT, the OCT has higher detection rate for retinal hamartoma in TSC patients; therefore, OCT might be promising for the clinical diagnosis of TSC.

**Key words:** Fundus Photography; Hamartoma; Infrared Imaging; Optical Coherence Tomography; Tuberous Sclerosis Complex

## Introduction

Tuberous sclerosis complex (TSC) is an autosomal dominant genetic disorder that causes benign tumors in multiple organs, including the eye, brain, skin, kidney, heart, and lung.[1,2] The epidemiological study shows that the incidence of TSC is approximately 1/6000.[3] TSC is caused by mutations of the *TSC1* or *TSC2* genes, which code for the tumor growth suppressors hamartin and tuberin, respectively.[3-5] TSC is commonly characterized by benign tumors called hamartomas in affected organs, and various signs and symptoms such as seizure, hypomelanotic macules, renal cysts, cardiac rhabdomyomas, and renal angiomyolipomas.[6]

Retinal hamartoma occurs in 40–50% of patients with TSC.[7] Retinal hamartoma may appear as a calcified multinodular lesion with a mulberry-like appearance or as a flat translucent whitish lesion.[8] Retinal hamartomas are commonly static, but aggressive growth has also been reported in some cases with associated complications such as macular edema, retinal detachment, and vitreous hemorrhage.[9] However, since TSC is a multiorgan disorder and the main clinical presentations

Access this article online

Quick Response Code:

Website: www.cmj.org

DOI: 10.4103/0366-6999.181976

**Address for correspondence:** Prof. Ning-Li Wang, Beijing Institute of Ophthalmology, Beijing Tongren Eye Center, Beijing Tongren Hospital, Capital Medical University, Beijing 100730, China
E-Mail: wningli@vip.163.com



**Received:** 15-01-2016 **Edited by:** Qiang Shi
**How to cite this article:** Bai DY, Wang X, Zhao JY, Li L, Gao J, Wang NL. Comparison of Color Fundus Photography, Infrared Fundus Photography, and Optical Coherence Tomography in Detecting Retinal Hamartoma in Patients with Tuberous Sclerosis Complex. Chin Med J 2016;129:1229-35.

are neurological disorders or skin lesions, retinal hamartomas are often misdiagnosed or the diagnosis is missed. Therefore, a sensitive method is required to detect retinal hamartomas in patients with TSC.

In this study, we analyzed 11 TSC patients for retinal hamartoma using color fundus photography, infrared fundus photography, and spectral-domain optical coherence tomography (SD-OCT). The sensitivities of these methods were compared for detecting retinal hamartoma in TSC patients, and the clinical manifestations and retinal features of these patients are summarized. In addition, *TSC1* and *TSC2* mutations were analyzed in eight patients to determine the genetic cause.

## Methods

### Patients

The study was approved by the Medical Ethics Committee of Beijing Children Hospital of the Capital University of Medical Science. Written informed consent was signed by the parents of all patients.

This study included 22 eyes of 11 patients (ten boys and one girl), who were diagnosed with TSC at the Departments of Ophthalmology and Neurology of Beijing Children Hospital between June 2014 and June 2015. TSC was diagnosed according to the criteria set by 2012 International Tuberous Sclerosis Complex Consensus Conference.[3] TSC can be diagnosed by the clinical manifestation profiles or gene examination (*TSC1* and *TSC2*) according to the National Institutes of Health Consensus Conference. The mean age of the patients was 8.0 ± 2.1 years (range: 4.1–10.8 years). Of the 11 patients, only one patient had a family history of TSC.

All patients underwent ophthalmologic, dermatologic, neurological, and stomatological examinations. All patients underwent magnetic resonance imaging (MRI; 3.0T, MAGNETOM Trio Tim Magnetic Resonance Imaging Equipment, Siemens, Germany), abdominal ultrasonography (MyLab70, Yum, Italy), and chest X-ray examinations.

### Ophthalmological examination

All patients underwent ophthalmological examinations including slit-lamp examination, color fundus photography, infrared fundus photography, and SD-OCT (Spectralis, Heidelberg Engineering, Germany) scanning included the circum papillary area (circle diameter, 3.4 mm), the macular area and nasal 15° retinal region. The scan protocol was volume scan with averaging 19 high-resolution frames per B-scan, 240 μm distance between each frame, and the scan scope was 20° × 15°. In some lesions, the single line scan may be used. All patients underwent cycloplegic autorefraction (with cyclopentolate hydrochloride eyedrops). Refractive error was defined as spherical equivalent (SE), the sum of spherical power and half-cylinder power in diopters. Myopia was defined as SE <−0.5 D, emmetropia was defined as −0.5 D≤ SE ≤0.5 D, and hyperopia was defined as SE >0.5 D.

Based on the morphological results of the fundus photography, retinal hamartomas were classified into three types as previously described by Zimmer-Galler and Robertson:[8] type I, a flat feathery pattern; type II, a mulberry-like pattern with calcified uplift; and type III, fundus morphology with the features of both types I and II.

### Genetic analysis

Genetic analyses were performed in eight TSC patients to identify *TSC1* and *TSC2* mutations, as previously reported.[10-12] Briefly, blood samples (2 ml) were collected from the median cubital vein of each patient and their parents and preserved in anticoagulation tubes. The genomic DNA was extracted from the peripheral blood using the phenol-chloroform extraction method. After the DNA extraction, the exons of *TSC1* and *TSC2* were analyzed using a neurocutaneous syndrome-related gene chip (Agilent, Santa Clara, CA, USA), and sequenced via a high-throughput sequencing method (HiSeq 2500, Illumina, San Diego, CA, USA).

### Statistical analysis

Statistical analyses were performed using the R Project for Statistical Computing (version 3.1.0, 2014; R Foundation for Statistical Computing, Vienna, Austria). Since there is no gold standard criteria for diagnosing hamartoma, Cohen's kappa test was used to compare the agreements among color fundus photography, infrared imaging (IFG), and OCT in detecting hamartoma. Larger value of kappa coefficient means better consistency and if kappa coefficient near zero means no consistency. The relative positive rates between any two methods were calculated and compared.

## Results

### Ophthalmological findings

The mean SE was −0.55 ± 1.42 D by autorefraction with cycloplegia. Of the 11 patients with TSC, hamartomas were found in 9, 7, and 7 patients via OCT, color fundus photography, and infrared fundus photography, respectively.

A total of 26 hamartomas were found. OCT was the most sensitive method to detect hamartomas [Figure 1]. All the 26 hamartomas were found by OCT, 18 by infrared fundus photography, and nine by color fundus photography [Table 1]. All the hamartomas that detected by color fundus photography or IFG can be detected in OCT. However, some hamartomas of early-stage showed in OCT cannot be detected by IFG or color fundus photography. Of the 11 patients, hamartomas occurred in bilateral eyes in seven, and in unilateral eye in two patients. OCT detected early-stage hamartomas that were invisible by fundus photography in three eyes of two cases. Specifically, in these cases OCT revealed abnormal thickening of the retinal nerve fiber layer, and extrusion of hamartomas into the inner layers of the retina and the retinal pigment

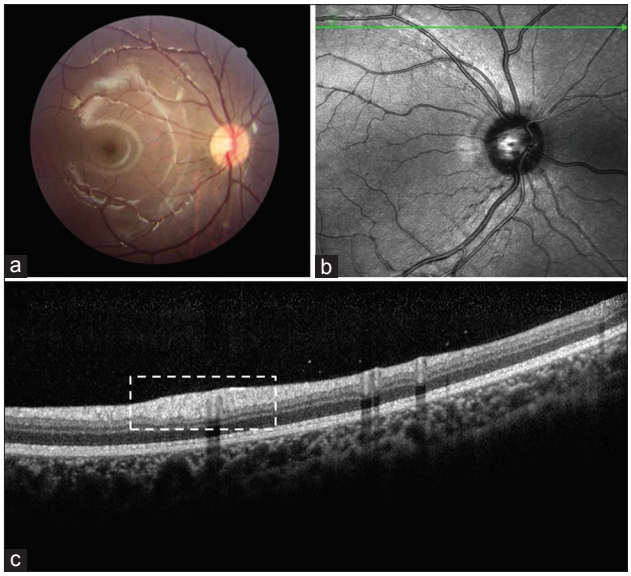


**Figure 1:** Retinal hamartoma in a patient with TSC. Retinal hamartoma was not detected by color fundus photography (a) or infrared fundus imaging (b). (c) OCT revealed abnormal thickening of the optic nerve fiber layer (rectangle). TSC: Tuberous sclerosis complex; OCT: Optical coherence tomography.

**Table 1: Hamartomas detected in 11 patients with TSC**

| Case | OCT (*n*) | | Infrared imaging (*n*) | | Fundus photography (*n*) | |
|---|---|---|---|---|---|---|
| | R | L | R | L | R | L |
| 1 | 0 | 2 | 0 | 1 | 0 | 1 |
| 2 | 2 | 1 | 2 | 1 | 0 | 1 |
| 3 | 2 | 2 | 2 | 1 | 1 | 1 |
| 4 | 2 | 1 | 0 | 0 | 0 | 0 |
| 5 | 0 | 0 | 0 | 0 | 0 | 0 |
| 6 | 0 | 1 | 0 | 1 | 0 | 1 |
| 7 | 1 | 3 | 1 | 2 | 1 | 0 |
| 8 | 1 | 1 | 0 | 0 | 0 | 1 |
| 9 | 2 | 2 | 2 | 2 | 1 | 1 |
| 10 | 1 | 2 | 1 | 2 | 0 | 0 |
| 11 | 0 | 0 | 0 | 0 | 0 | 0 |
| Total | 11 | 15 | 8 | 10 | 3 | 6 |

R: Right eye; L: Left eye; TSC: Tuberous sclerosis complex; OCT: Optical coherence tomography.

epithelium layer as well as the optic nerve [Figures 1 and 2]. In addition, with OCT characteristic features of some hamartomas were displayed, such as moth-eaten optically empty spaces (intralesional calcifications or intratumoral cavities) or areas of dot-like high reflectivity and low reflectivity, accompanied by disorganization of the inner layer retina structure and the retinal pigment epithelium layer [Figure 3]. In one patient with *TSC2* mutation and one hamartoma in the left eye, the patient had no systemic disorders, and hamartoma was the onset sign [Figure 4], he was diagnosed by gene examination. In addition, in one patient, one hamartoma was detected by OCT and color fundus photography, but not by infrared fundus imaging [Figure 5].

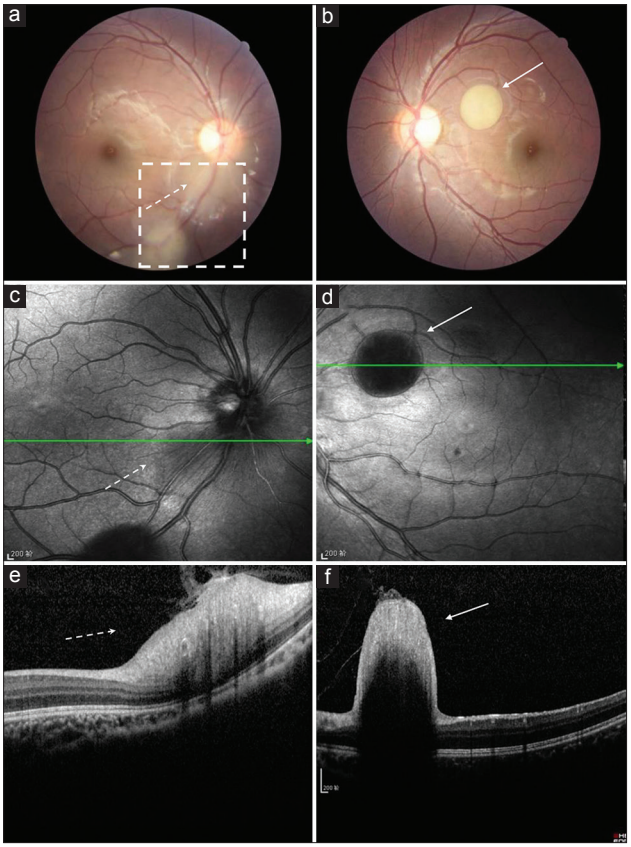


**Figure 2:** Retinal hamartoma occurred in bilateral eyes in a patient with TSC detected by color fundus photography (a and b), infrared fundus imaging (c and d), and OCT (e and f). a, c, and e indicates right eyes; b, d, and f indicates left eyes. The hamartomas in the left eye are very round and different from hamartomas in the right eye which look like epiretinal membrane (rectangle). The dotted arrows indicate the features of hamartomas includes dot-like hyper-reflectivity (e), the solid arrows show a low-reflective field under hyper-reflectivity (f). TSC: Tuberous sclerosis complex; OCT: Optical coherence tomography.

Nine hamartomas were detected in nine eyes of seven patients by color fundus photography, specifically: 5 type I in five eyes (55.6%) of five patients; 2 type II in two eyes (22.2%) of one patient; and 2 type III hamartomas in two eyes (22.2%) of one patient [Figure 6].

Cohen's kappa test was performed to test agreement among the three methods (color fundus photography, IFG, and OCT) in detecting hamartomas [Table 2]. The agreement between OCT and IFG was high relative to that between OCT and color fundus photography. The IFG/OCT positive rate for detecting hamartoma was the highest (69.2%), and the FHG/OCT positive rate for detecting hamartoma was the lowest (34.6%).

## Systemic diseases

Cases of systemic diseases such as skin lesions, neurological disorders, and visceral diseases occurred in 11 patients with TSC are as follows [Table 3]: epileptic seizure (8), hypomelanotic macules (9), enamel hypoplasia/hamartomas (1), subependymal nodules (10), cortical nodules (9), cardiac rhabdomyomas (5), renal angiomyolipomas (3), nonrenal hamartomas (3), and multiple renal cysts (5).

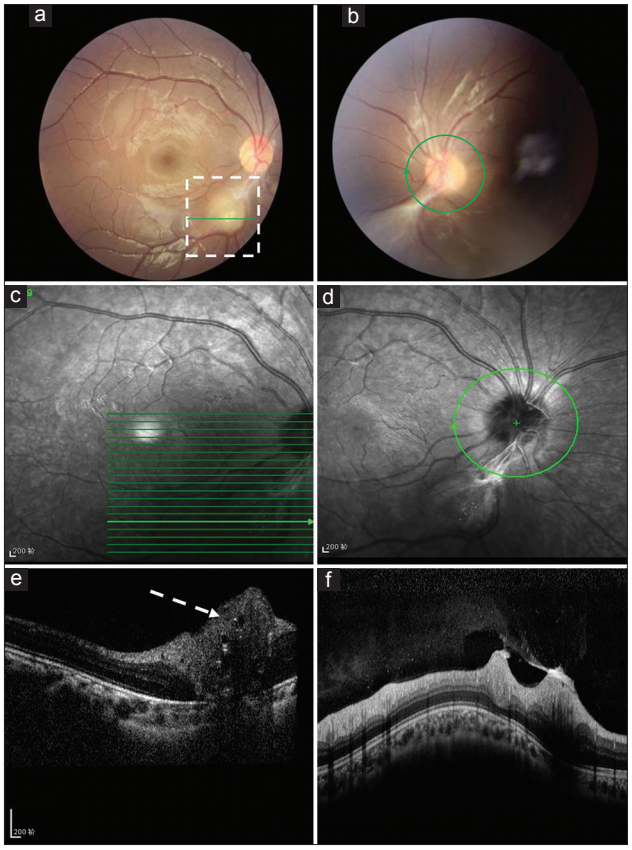


**Figure 3:** Retinal hamartoma occurred in bilateral eyes in a patient with TSC detected by color fundus photography (a and b), infrared fundus imaging (c and d), and OCT (e and f). a, c, and e indicates right eyes; b, d, and f indicates left eyes. The hamartoma shows in a rectangle and the green circle shows the circum papillary area scanning. Arrows indicate the features of hamartomas such as moth-eaten optically empty spaces. The hamartoma adheres to the vitreous cortex (f). TSC: Tuberous sclerosis complex; OCT: Optical coherence tomography.

**Table 2: Agreement among OCT, infrared imaging, and color fundus photography in detecting hamartoma by Cohen's kappa test**

| Items | Positive/ negative | Positive | Negative | Kappa coefficient |
|---|---|---|---|---|
| OCT/IFG | Positive | 18 | 8 | 0.59 |
| | Negative | 0 | 12 | |
| OCT/FHG | Positive | 9 | 17 | 0.25 |
| | Negative | 0 | 12 | |
| IFG/FHG | Positive | 8 | 10 | 0.40 |
| | Negative | 1 | 19 | |

OCT: Optical coherence tomography; IFG: Infrared imaging; FHG: Fundus photography.

### Tuberous sclerosis complex 1 and tuberous sclerosis complex 2 mutations

The genetic analyses of *TSC1* and *TSC2* mutations were performed in eight patients [Table 4]. Various mutations, including frameshift, termination, shear, and large fragment deletions were detected in these eight patients. *TSC1* mutations were found in one patient and *TSC2* mutations in six patients. One patient had no pathogenic *TSC1* or *TSC2* mutations. Four new mutations were first detected which have not been reported by the Human Gene Mutation Database (HGMD).

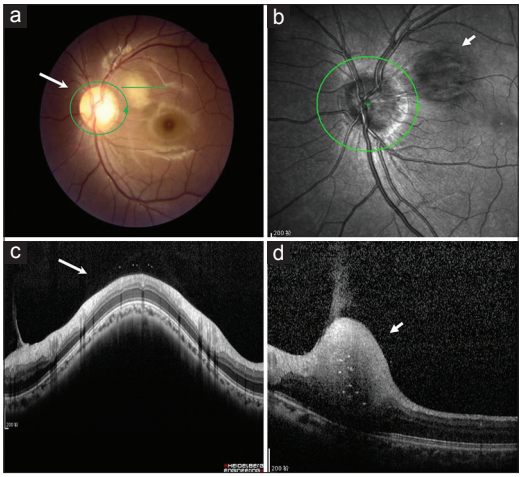


**Figure 4:** Hamartoma detected by color fundus photography (a), infrared fundus imaging (b), and OCT (c and d) in the left eye of a TSC patient with *TSC2* mutation, who had hamartoma as the onset sign without any systemic disease. The affected optic nerve with abnormal thickening is indicated in the circled area. The short arrow indicates areas of dot-like high reflectivity, and the retinal pigment epithelium layer was affected in hamartoma (d). OCT: Optical coherence tomography; TSC: Tuberous sclerosis complex.

## Discussion

In the present study, we compared the sensitivities of color fundus photography, infrared fundus photography, and OCT in detecting retinal hamartoma in 11 patients with TSC. We found more retinal hamartomas patients via OCT (9/11), but in only 7/11 patients when using either IFG or color fundus photography. All the hamartomas that detected by color fundus photography or IFG can be detected in OCT. However, some hamartomas of early-stage showed in OCT cannot be found by IFG or color fundus photography. Our study suggests that among these methods, OCT has the highest detection rate for retinal hamartoma in TSC patients, that is, higher than either IFG or color fundus photography. In addition, the incidence rate of retinal hamartoma detected by OCT in the present study is higher (9/11) than that reported in the literature (40–50%).[7] The following discussion includes a summary of the clinical manifestations and retinal features of these patients.

Color fundus photography is commonly used for detecting hamartoma in TSC patients. Since color fundus photography is not sensitive to detect early-stage hamartoma, this could lead to misdiagnoses. Misdiagnosis of lesions in the epiretinal membrane can also result from the uncooperative nature of children during the ophthalmological examination, and hamartoma can be confused with other retinal diseases such as retinoblastoma, which is the most common type of eye tumor in children. Other systemic symptoms such

as hypomelanotic macules and epilepsy, as well as cranial imaging, are important for the diagnosis of TSC.[6] However, in rare cases of TSC, retinal hamartoma can be the only sign.

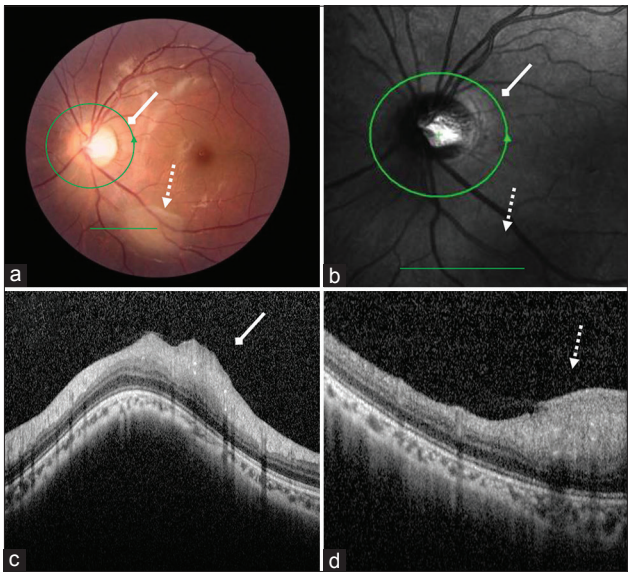


**Figure 5:** The dotted arrow shows one hamartoma in the left eye of a patient detected by color fundus photography (a) but not by infrared imaging (b). OCT (c and d) showed that the optic nerve shows dot-like high reflectivity in hamartoma and affected the outer nuclear layer lesion. Dashed arrows indicate lesions in circum papillary area. The solid arrow indicates that the hamartoma detected by color fundus photography and OCT but not detected by infrared imaging. OCT: Optical coherence tomography.

In the present study, we found one patient of *TSC2* only had retinal hamartoma without any systemic disorders.

In a single-center study of four patients with TSC, Xu *et al*.[13] reported that OCT and IFG detected early-stage hamartoma that was not detectable by fundus photography. In the present study, we also found that OCT and IFG are superior to fundus photography. In the 11 patients with TSC, 26 hamartomas were found by using OCT, IFG detected 18 hamartomas, and fundus photography identified only nine hamartomas. Based on our study, the most detecting rate of retinal hamartomas was OCT, then IFG, and then color fundus photography. In addition, we found that in one case, one hamartoma in the left eye was detected by OCT and fundus photography but not by infrared image. This suggests that IFG may also miss the detection of retinal hamartomas. Therefore, we recommend performing infrared scanning, and then OCT scanning of the whole retina, to identify retinal hamartomas in patients with TSC.

In a case series of 15 adult patients with TSC (mean age: 33 years), Shields *et al*.[14] found that type-III hamartoma accounted for 86.7% of all adult TSC patients, and type-II hamartomas occurred in 13.3% of all cases. In our present study, we found that type-I hamartoma occurred in 55.6%, and type-II and type-III each occurred in 22.2%. These studies suggest that type-I hamartoma is the predominant type of hamartomas in children and type III is the predominant type in adults.

Progression of retinal hamartoma from a noncalcified type I in children, to calcified type III in adults, may explain the

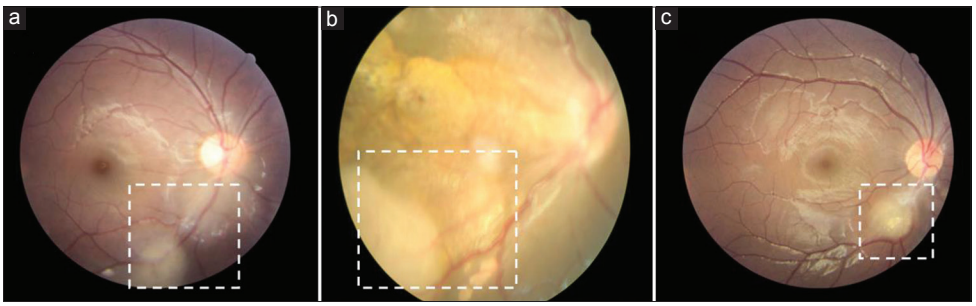


**Figure 6:** Three types of retinal hamartomas (rectangle) detected by color fundus photography. (a) Type-I retinal hamartomas. (b) Type-II retinal hamartomas. (c) Type-III retinal hamartomas.

**Table 3: Skin lesions, neurological disorders, and visceral diseases in 11 patients with tuberous sclerosis complex**

| Diseases | Patients | | | | | | | | | | | |
|---|---|---|---|---|---|---|---|---|---|---|---|---|
| | 1 | 2 | 3 | 4 | 5 | 6 | 7 | 8 | 9 | 10 | 11 | Total (*n*) |
| Epileptic seizures | − | − | + | + | + | − | + | + | + | + | + | 8 |
| Hypomelanotic macules | + | + | − | + | + | − | + | + | + | + | + | 9 |
| Enamel hypoplasia/hamartomas | − | − | − | − | − | − | − | − | − | + | − | 1 |
| Subependymal nodules | + | + | + | + | + | − | + | + | + | + | + | 10 |
| Cortical nodules | + | + | + | + | + | − | − | + | + | + | + | 9 |
| Cardiac rhabdomyomas | − | + | − | − | + | − | + | − | + | + | − | 5 |
| Renal angiomyolipomas | − | + | + | − | − | − | + | − | − | − | − | 3 |
| Nonrenal hamartomas | + | − | − | − | + | − | − | − | − | − | + | 3 |
| Multiple renal cysts | − | − | + | + | − | − | + | + | + | − | − | 5 |

**Table 4: Genetic analysis of eight children with TSC and their families**

| Patient | Mutated genes | Mutation | Exon | Nucleotide change | AA change | Report history | Family |
|---|---|---|---|---|---|---|---|
| 1 | *TSC1* | Termination | 19 | c.2371C>T | p.Q791X | PMID: 23728315 | None |
| 2 | *TSC2* | Frameshift | 18 | c.681delC | p.C227fs | None | None |
| 3 | *Neg* | – | – | – | – | – | None |
| 4 | *TSC2* | Frameshift | 39 | c.4982dupG | p.S1661fs | None | None |
| 5 | *TSC2* | Missense | 41 | c.5227C>T | p.R1743W | Medical Genetics 2006,7:72 | None |
| 6 | *TSC2* | Deletion | 22–31 | – | – | None | None |
| 7 | *TSC2* | Missense | 41 | c.5228G>A | p.R1743Q | PMID: 10732801 | None |
| 8 | *TSC2* | Splicing | 25 | c.2837+3A>G | Splicing | None | Father |

TSC: Tuberous sclerosis complex; AA: Amino acid; –: Not available.

difference between the present study and that of Shields *et al*.[14] In addition, since type-II hamartoma is similar to early-stage retinoblastoma in children, and it is difficult to distinguish retinal hamartoma from retinoblastoma based on fundus photography. Other symptoms such as skin lesions may be useful for differential diagnosis.

Furthermore, we found that hamartomas in children showed no obvious retinal edema or macular edema, which are often present in hamartomas in adults. Since early-stage retinal hamartomas that are not detected by fundus photography or IFG are identified by OCT scanning, we recommend that OCT-identified early-stage hamartoma that is invisible via fundus photography should be considered a new type of hamartoma in the classification of retinal hamartoma.

In the present study, we found that retinal hamartoma was derived from the retinal nerve fiber layer, and often affected all layers of the retina with the involvement of the optic nerve. Some of them also affect the vitreous cortex. Hamartomas around the optic nerve are difficult to identify, due to the thickening of the retinal nerve fiber layer. In hamartoma, dot-like high reflectivity can be present in the thickened nerve fiber layer, and lesions often affect the outer nuclear layer. Therefore, the presence of dot-like high reflectivity can assist in making the diagnosis of retinal hamartomas. Shields *et al*.[14] showed time-domain OCT (TD-OCT) findings of multifocal, round, confluent moth-eaten empty spaces with posterior shadowing in some patients. They pointed out that the empty spaces may represent either foci of calcification or intratumoral cavities. The calcification and cavities could be found on histopathology. However, the TD-OCT has been replaced by the SD-OCT technology, which provides faster scan speed, higher resolution, and potentially increased the accuracy of diagnose. In the present study, SD-OCT was used and the moth-eaten empty spaces with dot-like hyper-reflectivity were observed.

The wavelength of infrared scanning, OCT is 820 nm, 870 nm invisible laser and color fundus photography is visible light with multiple wavelengths. To date, the invisible light sources over 800 nm are used as the most of laser sources for retinal OCT. These near-infrared (NIR) laser sources can reduce the optical absorption of water, melanin, and blood and allow the excellent penetrating depth through the entire choroid and can focus one point. The visible light is not laser and cannot focus on one point with multiple wavelengths. Thus, compares to the visible light OCT, NIR OCT can increase the visibility of the outer retinal structures.[15] It can prove the limitation of visual light detecting retinal structure. Hence, we also proposed that color fundus photography detecting hamartoma is not sensitivity compared to OCT.

Rowley *et al*. found the SE −0.17 ± 2.09 D among eighty TSC patients with median age 27 years old (2–76 years old).[16] The SE was −0.55 ± 1.42 D with TSC children in our study. Choong *et al*. found the SE −1.11 ± 2.61 D among 117 children with age 7–12 years old from primary schools after cycloplegia.[17] Hence, the children with TSC had no significant difference in refractive status compared to others.

The genes *TSC1* and *TSC2* have been implicated in the pathogenesis of TSC.[3] *TSC2* mutations are more frequently identified in TSC patients than *TSC1* mutations.[18-20] Consistent with the literature, we found that *TSC2* mutations (6/8 patients) were more frequently present in TSC patients than *TSC1* mutations (1/8 patient).[18,19,21] Only one patient with retinal hamartoma carried no *TSC1* or *TSC2* mutation but can be diagnosed by clinical manifestations. In addition, in four of patients we report mutations that are new to the literature, and which are not contained in the HGMD.

In summary, we found that the predominant hamartoma was type I in children, the early-stage of hamartoma can be detected by OCT, compared with color fundus photography and IFG, OCT has higher detection rate for retinal hamartoma in patients with TSC.


## Financial support and sponsorship

Nil.


## Conflicts of interest

There are no conflicts of interest.

## References


1. Schwartz RA, Fernández G, Kotulska K, Józwiak S. Tuberous sclerosis complex: Advances in diagnosis, genetics, and management. J Am Acad Dermatol 2007;57:189-202. doi: 10.1016/j.jaad.2007.05.004.
2. Rodrigues DA, Gomes CM, Costa IM. Tuberous sclerosis complex. An Bras Dermatol 2012;87:184-96. doi: 10.1590/S0365-05962012000200001.
3. Krueger DA, Northrup H; International Tuberous Sclerosis Complex

Consensus Group. Tuberous sclerosis complex surveillance and management: Recommendations of the 2012 International Tuberous Sclerosis Complex Consensus Conference. Pediatr Neurol 2013;49:255-65. doi: 10.1016/j.pediatrneurol.2013.08.002.
4. Lawson JA, Chan CF, Chi CS, Fan PC, Kim HD, Kim KJ, *et al.* Managing tuberous sclerosis in the Asia-Pacific region: Refining practice and the role of targeted therapy. J Clin Neurosci 2014;21:1180-7. doi: 10.1016/j.jocn.2013.06.029.
5. van Slegtenhorst M, Nellist M, Nagelkerken B, Cheadle J, Snell R, van den Ouweland A, *et al.* Interaction between hamartin and tuberin, the TSC1 and TSC2 gene products. Hum Mol Genet 1998;7:1053-7. doi: 10.1093/hmg/7.6.1053.
6. Monteiro T, Garrido C, Pina S, Chorão R, Carrilho I, Figueiroa S, *et al.* Tuberous sclerosis: Clinical characteristics and their relationship to genotype/phenotype. An Pediatr (Barc) 2014;81:289-96. doi: 10.1016/j.anpedi.2014.03.022.
7. Leung AK, Robson WL. Tuberous sclerosis complex: A review. J Pediatr Health Care 2007;21:108-14. doi: 10.1016/j.pedhc.2006.05.004.
8. Zimmer-Galler IE, Robertson DM. Long-term observation of retinal lesions in tuberous sclerosis. Am J Ophthalmol 1995;119:318-24. doi: 10.1016/S0002-9394(14)71174-2.
9. Mennel S, Meyer CH, Peter S, Schmidt JC, Kroll P. Current treatment modalities for exudative retinal hamartomas secondary to tuberous sclerosis: Review of the literature. Acta Ophthalmol Scand 2007;85:127-32. doi: 10.1111/j.1600-0420.2006.00781.x.
10. Jang MA, Hong SB, Lee JH, Lee MH, Chung MP, Shin HJ, *et al.* Identification of TSC1 and TSC2 mutations in Korean patients with tuberous sclerosis complex. Pediatr Neurol 2012;46:222-4. doi: 10.1016/j.pediatrneurol.2012.02.002.
11. Mettin RR, Merkenschlager A, Bernhard MK, Elix H, Hirsch W, Kiess W, *et al.* Wide spectrum of clinical manifestations in children with tuberous sclerosis complex – Follow-up of 20 children. Brain Dev 2014;36:306-14. doi: 10.1016/j.braindev.2013.05.006.
12. Yamamoto T, Pipo JR, Feng JH, Takeda H, Nanba E, Ninomiya H, *et al.* Novel TSC1 and TSC2 mutations in Japanese patients with tuberous sclerosis complex. Brain Dev 2002;24:227-30. doi: 10.1016/S0387-7604(02)00017-7.
13. Xu L, Burke TR, Greenberg JP, Mahajan VB, Tsang SH. Infrared imaging and optical coherence tomography reveal early-stage astrocytic hamartomas not detectable by fundoscopy. Am J Ophthalmol 2012;153:883-9.e2. doi: 10.1016/j.ajo.2011.10.033.
14. Shields CL, Benevides R, Materin MA, Shields JA. Optical coherence tomography of retinal astrocytic hamartoma in 15 cases. Ophthalmology 2006;113:1553-7. doi: 10.1016/j.ophtha.2006.03.032.
15. Yi J, Chen S, Shu X, Fawzi AA, Zhang HF. Human retinal imaging using visible-light optical coherence tomography guided by scanning laser ophthalmoscopy. Biomed Opt Express 2015;6:3701-13. doi: 10.1364/BOE.6.003701.
16. Rowley SA, O'Callaghan FJ, Osborne JP. Ophthalmic manifestations of tuberous sclerosis: A population based study. Br J Ophthalmol 2001;85:420-3. doi: 10.1136/bjo.85.4.420.
17. Choong YF, Chen AH, Goh PP. A comparison of autorefraction and subjective refraction with and without cycloplegia in primary school children. Am J Ophthalmol 2006;142:68-74. doi: 10.1016/j.ajo.2006.01.084.
18. Jones AC, Shyamsundar MM, Thomas MW, Maynard J, Idziaszczyk S, Tomkins S, *et al.* Comprehensive mutation analysis of TSC1 and TSC2-and phenotypic correlations in 150 families with tuberous sclerosis. Am J Hum Genet 1999;64:1305-15. doi: 10.1086/302381.
19. Au KS, Williams AT, Roach ES, Batchelor L, Sparagana SP, Delgado MR, *et al.* Genotype/phenotype correlation in 325 individuals referred for a diagnosis of tuberous sclerosis complex in the United States. Genet Med 2007;9:88-100. doi: 10.1097GIM.0b013e31803068c7.
20. Niida Y, Lawrence-Smith N, Banwell A, Hammer E, Lewis J, Beauchamp RL, *et al.* Analysis of both TSC1 and TSC2 for germline mutations in 126 unrelated patients with tuberous sclerosis. Hum Mutat 1999;14:412-22. doi: 10.1002/(SICI)1098-1004(199911)14:5<412:AID-HUMU7>3.0.CO;2-K.
21. Nellist M, Brouwer RW, Kockx CE, van Veghel-Plandsoen M, Withagen-Hermans C, Prins-Bakker L, *et al.* Targeted next generation sequencing reveals previously unidentified TSC1 and TSC2 mutations. BMC Med Genet 2015;16:10. doi: 10.1186/s12881-015-0155-4.